J. Fluid Mech. (1990), *vol.* 214, *pp.* 17–42
Printed in Great Britain

On the instability of hypersonic flow past a wedge

By STEPHEN COWLEY[1] AND PHILIP HALL[2]
[1] Mathematics Department, Imperial College, London SW7 2BZ, UK
[2] Mathematics Department, Exeter University, Exeter, UK

(Received 29 November 1988 and in revised form 1 June 1989)

The instability of a compressible flow past a wedge is investigated in the hypersonic limit. Particular attention is paid to Tollmien–Schlichting waves governed by triple-deck theory though some discussion of inviscid modes is given. It is shown that the attached shock can have a significant effect on the growth rates of Tollmien–Schlichting waves. Moreover, the presence of the shock allows for more than one unstable Tollmien–Schlichting wave. Indeed an infinite discrete spectrum of unstable waves is induced by the shock, but these modes are unstable over relatively small but high frequency ranges. The shock is shown to have little effect on the inviscid modes considered by previous authors and an asymptotic description of inviscid modes in the hypersonic limit is given.

1. Introduction

Our concern is with the instability of hypersonic flow around a wedge of small angle. The work is motivated by recent interest in the development of hypersonic vehicles. We do not account for real gas effects even though some of the vehicles in question will certainly operate at speeds where such effects are important. Here we shall concentrate on Tollmien–Schlichting waves governed by triple-deck theory though some discussion of inviscid modes will be given. In a related paper, Hall & Fu (1989), the Görtler vortex instability mechanism at hypersonic speeds is considered. In that paper, it is shown that centrifugal instabilities have their structure simplified considerably in the hypersonic limit. This is not the case for Tollmien–Schlichting waves, although inviscid modes have a relatively simple structure. In fact, for a Chapman viscosity law we find that the logarithmically small layer at the edge of the boundary layer which controls inviscid modes is precisely the same layer where Görtler vortices become trapped at hypersonic speeds. It would therefore seem that the nonlinear interaction between inviscid and centrifugal instabilities is an important problem to be considered in the hypersonic limit.

Before giving more details of the problem to be considered here, we shall give a brief review of some relevant previous calculations on compressible stability problems. For a review of viscous and inviscid stability properties of compressible boundary layers the reader is referred to the articles by Reshotko (1976) and Mack (1987). Perhaps the main feature of compressible boundary layers of practical importance is that they are unstable to both inviscid and viscous instability waves. The inviscid modes have wavelengths comparable with the boundary-layer thickness whilst the Tollmien–Schlichting waves have longer wavelengths. Either the successive approximation procedure of Gaster (1974) or the formal asymptotic description based on triple-deck theory, as used for incompressible flows by Smith (1979*a*, *b*), can be extended to the compressible viscous instability problem in a routine manner.

Such a calculation was given by Gaponov (1981) using essentially Gaster's approach, whilst more recently Smith (1989) has applied triple-deck theory to the lower-branch viscous modes of compressible boundary layers (see Gajjar & Cole (1989) for a study of upper-branch modes in compressible flows). A significant result of Smith (1989) is that when the free-stream Mach number is increased there is a critical size of Mach number in terms of the (large) Reynolds number at which the Tollmien–Schlichting downstream development takes place on a lengthscale comparable with that over which the basic state develops. At this stage the waves cannot be described by any quasi-parallel theory and the evolution can only be described by numerical integration of the governing linear partial differential equations. This is precisely the situation in the incompressible Görtler stability problem, see Hall (1983); perversely, in the hypersonic limit the most significant Görtler vortices lose this property and become only weakly dependent on non-parallel effects. A question of some importance raised by Smith's work is whether the failure of the quasi-parallel approach at high Mach numbers means that many of the parallel flow calculations in this regime at finite Reynolds numbers are in error. Because Smith's prediction is based on a double high-Reynolds-number and high-Mach-number limit, the regime at which this failure occurs must be identified by numerical integration of the governing linear partial differential equations.

This inviscid modes of instability of a compressible boundary layer have been documented by Mack (1987). In fact, there can be unstable two- and three-dimensional modes and neutral modes associated with a generalized inflection point and non-inflectional neutral modes. At Mach numbers above three it is the inviscid modes which have the highest growth rates and therefore presumably dominate the transition problem in compressible boundary layers. However, previous calculations for viscous and inviscid modes have taken little account of the presence of shocks in the flow field (but see Petrov 1984), though at high Mach numbers there is no question that they play an important role in determining the basic state. A primary aim of the present calculation is to gain some insight into the role of shock waves in the formation of viscous and inviscid modes in a compressible boundary layer.

The particular configuration that we investigate is the hypersonic flow around an aligned wedge of semi-angle θ. The inviscid flow in this case is a uniform state either side of straight shocks which make an angle $\phi = \sigma - \theta$ with the wedge. At the wedge a boundary layer is set up and the fluid velocity is reduced to zero inside this layer. We restrict our attention to the case when the wedge is insulated though our calculations can readily be extended to the isothermal case.

In order that Tollmien–Schlichting wave disturbances to this flow can be treated in a quasi-parallel manner we make the Newtonian approximation and take the distance of the shock from the wall to be comparable with the upper-deck scale over which Tollmien–Schlichting waves governed by triple-deck theory will decay. At the shock we derive linearized boundary conditions which the Tollmien–Schlichting wave must satisfy. This condition effectively changes the eigenrelation from that discussed in the absence of shocks by Smith (1989). We show that the shock has a significant effect on the growth rate of the so-called subsonic mode discussed by Smith, and further, that additional modes exist because of the shock. The latter modes can be interpreted as acoustic waves trapped between the wedge and the shock. Some have much larger growth rates than the subsonic mode, although it is noted that such modes have relatively high frequencies and are unstable only over short ranges of frequency.

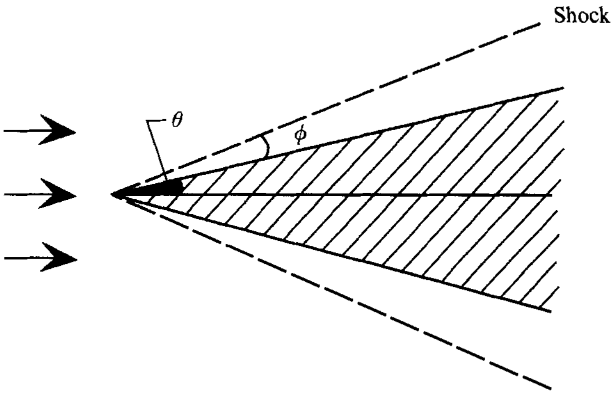

FIGURE 1. The geometry of the wedge and shock for a high-Mach-number flow.

Some discussion of inviscid disturbances is also given. At high Mach numbers we give the appropriate asymptotic structure of the so-called acoustic modes, and show that except for very small wedge angles they will be influenced little by the presence of the shock.

The procedure adopted in the rest of this paper is as follows: in §2 we formulate the appropriate scalings for Tollmien–Schlichting instabilities of the hypersonic flow past a wedge. In §3 the triple-deck equations for such modes are derived and in §4 the dispersion relationship appropriate to the linearized form of these equations is given and discussed. In §5 we give a brief discussion of the structure of inviscid modes in hypersonic boundary layers whilst in §6 we draw some conclusions. Finally in an Appendix we derive the shock conditions appropriate to a disturbance with arbitrary lengthscales and use them to find the simplified shock condition for a Tollmien–Schlichting wave.

2. Formulation

The basic flow whose stability we examine is illustrated in figure 1. For simplicity, the wedge is taken to be symmetrically aligned with an oncoming supersonic flow with velocity magnitude $\hat{U}$. Shocks of semi-angle σ develop from the tip of the wedge (the acute angle between the shock and the wedge is $\phi = \sigma - \theta$). Quantities upstream of the shock are indicated by the subscript u, and quantities in the so-called 'shock-layer' between the shock and wedge by the subscript s. Cartesian axes are introduced with the $\hat{x}$- and $\hat{y}$-coordinates aligned and normal with the upper surface of the wedge, and the $\hat{z}$-coordinate in the spanwise direction. The corresponding velocity components are $\hat{\boldsymbol{u}} = (\hat{u}, \hat{v}, \hat{w})$, while $\hat{t}$, $\hat{\rho}$, $\hat{p}$, $\hat{T}$ and $\hat{h}$ are used to denote time, density, pressure, temperature and enthalpy respectively. We shall assume that the fluid is a perfect gas with ratio of specific heats γ; then the upstream Mach number, M_u, is given by

$$M_u = \frac{\hat{U}}{a_u}, \tag{2.1a}$$

where the sound speed a_u is given by

$$a_u^2 = \frac{\gamma \hat{p}_u}{\hat{\rho}_u} = (\gamma - 1)\,\hat{h}_u. \tag{2.1b}$$

The inviscid solution for this flow configuration consists of uniform quantities on either sides of straight shocks (e.g. see Hayes & Probstein 1966). Specifically,

$$\epsilon = \frac{\hat{\rho}_u}{\hat{\rho}_s} = \left(\frac{\gamma-1}{\gamma+1}\right)\left(1+\frac{2}{(\gamma-1)M_u^2\sin^2\sigma}\right), \tag{2.2a}$$

$$\frac{\hat{p}_s}{\hat{p}_u} = 1+\gamma M_u^2 \sin^2\sigma(1-\epsilon), \tag{2.2b}$$

$$\frac{\hat{h}_s}{\hat{h}_u} = 1+\tfrac{1}{2}(\gamma-1)(1-\epsilon^2)M_u^2\sin^2\sigma, \tag{2.2c}$$

$$\tan\phi = \epsilon\tan\sigma, \tag{2.2d}$$

$$(\hat{u}_\parallel)_u = (\hat{u}_\parallel)_s = \hat{U}\cos\sigma, \quad (\hat{u}_\perp)_u = -\hat{U}\sin\sigma, \quad (\hat{u}_\perp)_s = -\epsilon\hat{U}\sin\sigma, \tag{2.2e}$$

where $\hat{u}_\parallel$ and $\hat{u}_\perp$ are the velocity components parallel and perpendicular to the shock. From (2.1) it follows that between the shock and the wedge the fluid velocity has magnitude

$$\hat{U}_s = \hat{U}\cos\sigma(1+\epsilon^2\tan^2\sigma)^{\frac{1}{2}}, \tag{2.3}$$

and the local Mach number M_s is given by

$$M_s^2 = \frac{M_u^2\cos^2\sigma(1+\epsilon^2\tan^2\sigma)}{1+\frac{1}{2}(\gamma-1)(1-\epsilon^2)M_u^2\sin^2\sigma}, \tag{2.4a}$$

or equivalently

$$M_u^2 = \frac{M_s^2}{\cos^2\sigma(1+\epsilon^2\tan^2\sigma)-\frac{1}{2}(\gamma-1)(1-\epsilon^2)M_s^2\sin^2\sigma}. \tag{2.4b}$$

Note that (2.3) specifies the slip velocity along the wedge, which in viscous flow necessitates the existence of a boundary layer.

Before examining this boundary layer in detail we introduce a non-dimensionalization based on the flow quantities between the shock and the wedge, and a lengthscale L which is the distance of interest from the tip of the wedge. Specifically, we introduce coordinates $L\boldsymbol{x}$, velocities $\hat{U}_s\boldsymbol{u}$, time $Lt/\hat{U}_s$, pressure $\hat{\rho}_s\hat{U}_s^2 p$, density $\hat{\rho}_s\rho$, temperature $\hat{T}_s T$ and enthalpy $\hat{h}_s h$. The governing equations of the flow then become

$$\frac{\partial\rho}{\partial t}+\nabla\cdot(\rho\boldsymbol{u}) = 0, \tag{2.5a}$$

$$\rho\frac{D\boldsymbol{u}}{Dt} = -\nabla p+\frac{1}{Re}[2\nabla\cdot(\mu\boldsymbol{e})+\nabla((\mu'-\tfrac{2}{3}\mu)\nabla\cdot\boldsymbol{u})], \tag{2.5b}$$

$$\rho\frac{DT}{Dt} = (\gamma-1)M_s^2\frac{Dp}{Dt}+\frac{1}{Pr\,Re}\nabla\cdot(\mu\nabla T)+\frac{(\gamma-1)M_s^2}{Re}\Phi, \tag{2.5c}$$

$$\gamma M_s^2 p = \rho T, \quad h = T, \tag{2.5d, e}$$

where

$$e_{ij} = \frac{1}{2}\left(\frac{\partial u_i}{\partial x_j}+\frac{\partial u_j}{\partial x_i}\right), \tag{2.6a}$$

$$\Phi = 2\mu\boldsymbol{e}:\boldsymbol{e}+(\mu'-\tfrac{2}{3}\mu)(\nabla\cdot\boldsymbol{u})^2. \tag{2.6b}$$

Here μ and μ' are the shear and bulk viscosities respectively, both of which have been non-dimensionalized by a typical viscosity $\hat{\mu}_s$, Pr is the constant Prandtl number, and

$$Re = \frac{\hat{\rho}_s \hat{U}_s L}{\hat{\mu}_s} \tag{2.6c}$$

is the Reynolds number which we shall assume is large. Henceforth, the subscript s will be omitted from M_s. For completeness here we define coordinates (ξ, η, z), where ξ, η measure distance along and normal to the shock:

$$\xi = x\cos\phi + y\sin\phi, \quad \eta = -x\sin\phi + y\cos\phi. \tag{2.7}$$

These coordinates will be used in the Appendix.

Similarity solutions to the steady boundary-layer equations can be found in terms of the Dorodnitsyn–Howarth variable (e.g. Stewartson 1964). For simplicity we shall assume (i) that the wedge walls are insulating, i.e. $\partial T/\partial y = 0$ on $y = 0$, and (ii) that the Prandtl number is unity, i.e. $Pr = 1$. The temperature at the wall, T_w, is then given by (e.g. Stewartson 1964)

$$T_w = 1 + \tfrac{1}{2}(\gamma - 1)M^2. \tag{2.8}$$

The linear stability of this boundary-layer flow has been extensively studied using the Orr–Sommerfeld quasi-parallel approximation (e.g. Mack 1969, 1984, 1987). Recently, Smith (1989) has shown how an asymptotic triple-deck description of lower-branch Tollmien–Schlichting waves (i.e. 'first mode' waves) can be obtained for wave directions sufficiently oblique to be outside the local wave-Mach-cone direction. In the limit of large Mach number M, Smith (1989) found that the most rapidly growing waves have frequencies of order $Re^{\frac{1}{4}}\mu_w^{-\frac{1}{4}}T_w^{-\frac{3}{4}}M^{-\frac{1}{2}}$, and wavelengths in the x- and z-directions of order

$$Re^{-\frac{3}{8}}\mu_w^{\frac{3}{8}}T_w^{\frac{9}{8}}M^{\frac{3}{4}}, \quad Re^{-\frac{3}{8}}\mu_w^{\frac{3}{8}}T_w^{\frac{9}{8}}M^{-\frac{1}{4}} \tag{2.9a, b}$$

respectively, where μ_w is the viscosity coefficient at the wall, and we have slightly modified Smith's (1989) results to account for the case when the shear viscosity is not given by Chapman's law (see also Blackaby 1990). As is conventional there are lower, middle, and upper decks in the y-direction with scales

$$Re^{-\frac{5}{8}}\mu_w^{\frac{5}{8}}T_w^{\frac{7}{8}}M^{\frac{1}{4}}, \quad Re^{-\frac{1}{2}}\mu_w^{\frac{1}{2}}T_w^{\frac{1}{2}}, \quad Re^{-\frac{3}{8}}\mu_w^{\frac{3}{8}}T_w^{\frac{9}{8}}M^{-\frac{1}{4}} \tag{2.9c, d, e}$$

respectively.

One aim of this paper is to see how the growth rates of these oblique Tollmien–Schlichting waves are modified by the presence of a shock. To this end, we attempt to scale the problem so that the shock occurs in the upper deck. Thus, since ϕ must be small, it follows from (2.2d) and (2.9e) that

$$\phi \sim \epsilon \tan\sigma \sim Re^{-\frac{3}{8}}\mu_w^{\frac{3}{8}}T_w^{\frac{9}{8}}M^{-\frac{1}{4}}, \tag{2.9f}$$

which from (2.9a) implies an x lengthscale of order $M\epsilon\tan\sigma$. If the complications arising from non-parallel effects are to be excluded in order to concentrate on the effects of the shock interaction, we require

$$M\epsilon\sigma \ll 1, \tag{2.10a}$$

i.e. that the wavelength of the Tollmien–Schlichting waves is much less than the distance from the apex of the wedge; here we have assumed that $\sigma \ll 1$, as turns out to be necessary (see (2.16d, e)). From (2.2a) and (2.4a), $\epsilon = O(M^{-2}\sigma^{-2})$, so (2.10$a$) becomes

$$\sigma M \gg 1. \tag{2.10b}$$

However, for $M_u^2 > 0$ in (2.4b) we require, since $\epsilon \ll 1$,

$$(\gamma - 1)M^2\sigma^2 < 2. \tag{2.10c}$$

Hence, in order to consider the effect of the shock on the instability waves without the effects of non-parallelism we are *forced* to make the 'Newtonian' assumption

$$(\gamma - 1) \ll 1. \tag{2.11}$$

It follows that when $(\gamma - 1)$ is not small there is no systematic asymptotic approach to this problem that allows the inclusion of shock effects without those associated with non-parallelism.

Before proceeding to asymptotic expansions based on the above scalings, it is convenient to consider whether there are any further restrictions on the magnitudes of $(\gamma - 1)$, M and σ. First, we note that a pressure/acoustic wave incident on a shock will produce entropy and shear waves as well as generating a reflected wave. The entropy/shear waves have a typical lengthscale normal to the shock of magnitude

$$\epsilon\sigma\bar{\alpha}^{-1}, \tag{2.12}$$

where $\bar{\alpha}$ is a typical wavenumber in the x-direction (see §3 below); from (2.9a, f) $\bar{\alpha} \sim M\sigma$. For simplicity we choose to ignore viscous effects in these waves at leading order, in which case we require

$$\epsilon\sigma\bar{\alpha}^{-1} \gg (\bar{\alpha}Re)^{-\frac{1}{2}}, \quad \text{i.e.} \quad \sigma^3 M^5 \ll Re. \tag{2.13}$$

If it is assumed that the shock has a viscous internal structure, then its thickness is order $(\epsilon\sigma Re)^{-1}$ (e.g. Moore 1963), and (2.13) then ensures that the entropy/shear waves have a wavelength much larger than the thickness of the shock. It follows from (2.10a) that these waves have typical y-scales much less than the width of the upper deck.

Since nonlinear effects are an important part in transition to turbulence, we shall select a scaling which leads to a nonlinear problem, before linearizing to obtain an analytic solution. Following the scalings in Smith (1989), we conclude that a nonlinear lower-deck problem is recovered if

$$p \sim Re^{-\frac{1}{4}}\mu_w^{\frac{1}{4}}T_w^{-\frac{1}{4}}M^{-\frac{3}{2}}. \tag{2.14a}$$

In the upper deck this generates a velocity perturbation normal to the wedge (and normal to the shock) of order $Re^{-\frac{1}{4}}\mu_w^{\frac{1}{4}}T_w^{-\frac{1}{4}}M^{-\frac{1}{2}}$. In order that linearized shock conditions are applicable, the undisturbed velocity normal to the shock should be much larger than this, i.e. from (2.2e)

$$\epsilon\sigma \gg Re^{-\frac{1}{4}}\mu_w^{\frac{1}{4}}T_w^{-\frac{1}{4}}M^{-\frac{1}{2}}, \quad \text{i.e.} \quad \sigma^4 M^6 \ll Re\,\mu_w^{-1}T_w. \tag{2.14b}$$

If this condition is violated, nonlinear entropy waves result, a difficulty which is not tackled here. Also, note that if (2.15) is satisfied, then from (2.10b) so is (2.13).

In order to fix a scaling we shall assume that (cf. (2.10c))

$$(\gamma - 1)M^2\sigma^2 \sim 1. \tag{2.15a}$$

Since $\sigma \ll 1$ (see below), it follows from (2.8) that $T_{\mathrm{w}} \sim (\gamma-1)M^2 \gg 1$; hence the temperature variation in the undisturbed boundary layer is large. It is also necessary to fix the viscosity law. For Chapman's law $\mu_{\mathrm{w}} = CT_{\mathrm{w}}$, while for Sutherland's law

$$\mu_{\mathrm{w}} = \frac{1+\bar{C}}{T_{\mathrm{w}}+\bar{C}} T_{\mathrm{w}}^{\frac{3}{2}} \approx (1+\bar{C})\, T_{\mathrm{w}}^{\frac{1}{2}}.$$

With these assumptions, the interaction condition (2.9*f*) becomes

$$M \sim \sigma^{\frac{8}{7}} Re^{\frac{3}{14}}\,\text{(Chapman)}, \quad M \sim \sigma^{\frac{13}{14}} Re^{\frac{3}{14}}\,\text{(Sutherland)}. \tag{2.15b, c}$$

The restrictions (2.10*b*) and (2.14) imply

$$Re^{-\frac{1}{10}} \ll \sigma \ll Re^{-\frac{1}{38}}, \quad \text{i.e.} \quad Re^{\frac{1}{10}} \ll M \ll Re^{\frac{7}{38}} \quad \text{(Chapman)}, \tag{2.15d}$$

$$Re^{-\frac{1}{9}} \ll \sigma \ll Re^{-\frac{1}{37}}, \quad \text{i.e.} \quad Re^{\frac{1}{9}} \ll M \ll Re^{\frac{7}{37}} \quad \text{(Sutherland)}. \tag{2.15e}$$

If the lower-deck is forced to remain linear then the upper bound on σ relaxes to $\sigma \ll Re^{-\frac{1}{122}}$ and $\sigma \ll Re^{-\frac{1}{107}}$ for the two laws respectively. In (2.15*d*, *e*) the lower bound is attained when the quasi-parallel assumption is violated (Smith 1989; Blackaby 1990), which for our scaling requires $(\gamma-1) \sim 1$. In particular, (2.15*d*) does not violate Smith's (1989) restriction on the Mach number for the quasi-parallel assumption since he assumes that $(\gamma-1)$ is strictly order one, whereas we take $(\gamma-1) \ll 1$. However if $(\gamma-1) \sim 1$, the above arguments indicate that for the non-parallel scaling, i.e. for $M \sim Re^{\frac{1}{10}}$ in the case of Chapman's law, the effects of an outer-deck shock need to be included unless $\sigma \gg M^{-1}$. We also note that because we take $(\gamma-1) \ll 1$, there is no strong interaction between the shock and the undisturbed boundary layer for the range of Mach numbers specified by (2.15*d*, *e*) (cf. Brown, Stewartson & Williams 1975).

For convenience we introduce the scalings

$$\sigma = \Sigma M^{\frac{7}{8}} Re^{-\frac{3}{16}}\,\text{(Chapman)}, \quad \sigma = \Sigma M^{\frac{14}{13}} Re^{-\frac{3}{13}}\,\text{(Sutherland)}, \tag{2.16a, b}$$

$$(\gamma-1)M^2\sigma^2 = \Gamma\Sigma^2, \tag{2.16c}$$

then

$$T_{\mathrm{w}} \approx \tfrac{1}{2}\Gamma\Sigma^2\sigma^{-2} \gg 1, \tag{2.16d}$$

and to satisfy (2.10*c*) we require $\Gamma\Sigma^2 < 2$. Also, from (2.2*d*), (2.4*b*) and (2.16) the position of the shock is given by

$$y = x\epsilon \tan\sigma \approx Re^{\frac{3}{16}} M^{-\frac{23}{8}} \Sigma^{-1} x \quad \text{(Chapman)}, \tag{2.17a}$$

$$y = x\epsilon \tan\sigma \approx Re^{\frac{3}{13}} M^{-\frac{40}{13}} \Sigma^{-1} x \quad \text{(Sutherland)}, \tag{2.17b}$$

since

$$\epsilon \approx \frac{1}{\sigma^2 M^2}.$$

3. The triple-deck equations

The scalings leading to these equations for compressible flow have been given elsewhere (e.g. Stewartson 1974); hence only a brief outline is given here. In all three decks the x-, z- and t-scalings are

$$\left.\begin{aligned} x &= 1+Re^{-\frac{3}{8}}\mu_{\mathrm{w}}^{\frac{3}{8}}\, T_{\mathrm{w}}^{\frac{9}{8}} M^{\frac{3}{4}} \lambda^{-\frac{5}{4}} X, \quad z = Re^{-\frac{3}{8}}\mu_{\mathrm{w}}^{\frac{3}{8}}\, T_{\mathrm{w}}^{\frac{9}{8}} \lambda^{-\frac{5}{4}} M^{-\frac{1}{4}} Z, \\ t &= Re^{-\frac{1}{4}}\mu_{\mathrm{w}}^{\frac{1}{4}}\, T_{\mathrm{w}}^{\frac{9}{4}} M^{\frac{1}{2}} \lambda^{-\frac{3}{2}} \tau, \end{aligned}\right\} \tag{3.1}$$

where λ is boundary-layer skin friction from the undisturbed middle-deck solution (for Chapman's viscosity law $\lambda = 0.332$, i.e. the Blasius value).

3.1. *Lower deck*

In this layer, the scalings are

$$\left.\begin{aligned} y &= Re^{-\frac{5}{8}}\mu_w^{\frac{5}{8}}T_w^{\frac{7}{8}}M^{\frac{1}{4}}\lambda^{-\frac{3}{4}}Y, \quad u \sim Re^{-\frac{1}{8}}\mu_w^{\frac{1}{8}}T_w^{\frac{3}{8}}M^{\frac{1}{4}}\lambda^{\frac{1}{4}}U, \\ v &\sim Re^{-\frac{3}{8}}\mu_w^{\frac{3}{8}}T_w^{\frac{1}{8}}M^{-\frac{1}{4}}\lambda^{\frac{3}{4}}V, \quad w \sim Re^{-\frac{1}{8}}\mu_w^{\frac{1}{8}}T_w^{\frac{3}{8}}M^{-\frac{3}{4}}\lambda^{\frac{1}{4}}W, \\ p &\sim M^{-2}+Re^{-\frac{1}{4}}\mu_w^{\frac{1}{4}}T_w^{-\frac{1}{4}}M^{-\frac{3}{2}}\lambda^{\frac{1}{2}}P, \quad T \sim T_w, \quad \rho \sim T_w^{-1}. \end{aligned}\right\} \tag{3.2}$$

On substituting into (2.5) we obtain at leading order

$$\left.\begin{aligned} U_X+V_Y+W_Z &= 0, \quad P_Y = 0, \\ U_\tau+UU_X+VU_Y+WU_Z &= U_{YY}, \\ W_\tau+UW_X+VW_Y+WW_Z &= -P_Z+W_{YY}. \end{aligned}\right\} \tag{3.3}$$

The boundary conditions are

$$\left.\begin{aligned} U = V = W = 0 \quad &\text{on} \quad Y = 0, \\ U \to Y+A(X,Z,\tau), \quad W \to 0 \quad &\text{as} \quad Y \to \infty, \end{aligned}\right\} \tag{3.4}$$

where the conditions as $Y \to \infty$ come from matching with the middle deck, and A is the so-called displacement function.

3.2. *Middle deck*

The middle deck has the same thickness as the undisturbed boundary layer, which has a finite extent in y when $T_w \gg 1$ (although an infinite extent in terms of the Dorodnitsyn–Howarth variable). Strictly this means that the middle deck should be divided into three regions (i) a boundary-layer region where $T \gg 1$, (ii) a region where $T \sim 1$, and (iii) a small transition region between the two.

In region (i) the standard scalings and solutions apply:

$$\left.\begin{aligned} y &= Re^{-\frac{1}{2}}\mu_w^{\frac{1}{2}}T_w^{\frac{1}{2}}y^*, \quad u \sim u_0^*(y^*)+Re^{-\frac{1}{8}}\mu_w^{\frac{1}{8}}T_w^{\frac{3}{8}}M^{\frac{1}{4}}\lambda^{-\frac{3}{4}}Au^*_{0y^*}, \\ v &\sim -Re^{-\frac{1}{4}}\mu_w^{\frac{1}{4}}T_w^{-\frac{1}{4}}M^{-\frac{1}{2}}\lambda^{\frac{1}{2}}A_X u_0^*, \quad w \sim Re^{-\frac{1}{4}}\mu_w^{\frac{1}{4}}T_w^{-\frac{1}{4}}M^{-\frac{1}{2}}\lambda^{\frac{1}{2}}(R_0^* u_0^*)^{-1}D(X,Z,\tau), \\ p &\sim M^{-2}+Re^{-\frac{1}{4}}\mu_w^{\frac{1}{4}}T_w^{-\frac{1}{4}}M^{-\frac{3}{2}}\lambda^{\frac{1}{2}}P, \quad \rho \sim R_0^*(y^*)+Re^{-\frac{1}{8}}\mu_w^{\frac{1}{8}}T_w^{\frac{3}{8}}M^{\frac{1}{4}}\lambda^{-\frac{1}{4}}AR^*_{0y^*}, \end{aligned}\right\} \tag{3.5}$$

where $u_0^*(y^*)$ and $R_0^*(y^*)$ are the undisturbed velocity and density profiles respectively (note that $R_0^* = O(T_w^{-1})$), and $D_X = -P_Z$.

Essentially the same solution holds in regions (ii) and (iii), although minor rescalings are necessary. For example in region (ii) $R_0^* = u_0^* = 1$, which leads to simplifications in the expressions for u and ρ in particular. The precise scaling in region (iii) depends on the viscosity law. For example, in the case of the Chapman law, $u^*_{0y^*}$ scales with $(\log T_w)^{\frac{1}{2}}$ with the result that the largest velocity perturbations occur in this region. Thus for M close to $R^{\frac{1}{10}}$ the middle deck may become nonlinear for smaller wave amplitudes than the lower deck.

3.3. *Upper deck*

The scalings for the pressure/acoustic waves here are

$$y = Re^{-\frac{3}{8}}\mu_{\mathrm{w}}^{\frac{3}{8}}T_{\mathrm{w}}^{\frac{9}{8}}M^{-\frac{1}{4}}\lambda^{-\frac{5}{4}}\bar{y}, \quad u \sim 1+Re^{-\frac{1}{4}}\mu_{\mathrm{w}}^{\frac{1}{4}}T_{\mathrm{w}}^{-\frac{1}{4}}M^{-\frac{3}{2}}\lambda^{\frac{1}{2}}\bar{u}_1, \qquad (3.6a, b)$$

$$(v, w) \sim Re^{-\frac{1}{4}}\mu_{\mathrm{w}}^{\frac{1}{4}}T_{\mathrm{w}}^{-\frac{1}{4}}M^{-\frac{1}{2}}\lambda^{\frac{1}{2}}(\bar{v}_1, \bar{w}_1), \quad p \sim M^{-2}+Re^{-\frac{1}{4}}\mu_{\mathrm{w}}^{\frac{1}{4}}T_{\mathrm{w}}^{-\frac{1}{4}}M^{-\frac{3}{2}}\lambda^{\frac{1}{2}}\bar{p}_1, \quad (3.6c, d)$$

$$\rho \sim 1+Re^{-\frac{1}{4}}\mu_{\mathrm{w}}^{\frac{1}{4}}T_{\mathrm{w}}^{-\frac{1}{4}}M^{\frac{1}{2}}\lambda^{\frac{1}{2}}\bar{\rho}_1, \quad T \sim 1+(\gamma-1)Re^{-\frac{1}{4}}\mu_{\mathrm{w}}^{\frac{1}{4}}T_{\mathrm{w}}^{-\frac{1}{4}}M^{\frac{1}{2}}\lambda^{\frac{1}{2}}\bar{T}_1. \quad (3.6e, f)$$

These yield the governing equation for the pressure

$$\bar{p}_{1XX}-\bar{p}_{1\bar{y}\bar{y}}-\bar{p}_{1ZZ} = 0. \qquad (3.7)$$

One boundary condition comes from matching with the middle deck, i.e.

$$\bar{p}_{1\bar{y}} = A_{XX} \quad \text{on} \quad \bar{y} = 0 \qquad (3.8)$$

(note $\bar{p}_1 = P$ on $\bar{y} = 0$), while another boundary condition is to be applied at the shock at

$$\bar{y} = \bar{y}_{\mathrm{s}} = \left(\frac{2}{\Gamma}\right)^{\frac{3}{4}}\frac{\lambda^{\frac{5}{4}}}{C^{\frac{3}{8}}\Sigma} \quad \text{(Chapman)}, \qquad (3.9a)$$

$$\bar{y} = \bar{y}_{\mathrm{s}} = \left(\frac{2}{\Gamma}\right)^{\frac{21}{16}}\frac{\lambda^{\frac{5}{4}}}{(1+\bar{C})^{\frac{3}{8}}\Sigma} \quad \text{(Sutherland)}. \qquad (3.9b)$$

As is conventional, solutions to (3.7) will be referred to as acoustic waves.

3.4. *Shock conditions*

Wave transmission and reflection across shocks have been studied by Moore (1954), Ribner (1954), McKenzie & Westphal (1968) and others. In general, whenever an acoustic wave is incident on a shock, entropy and vorticity waves are generated in addition to a reflected/transmitted acoustic wave. The entropy/vorticity waves have the same frequency and the same wavelengths parallel to the shock as the acoustic waves. However, they propagate in the direction of the mean flow, which means for the present scalings that their wavelengths normal to the shock are very much less than the acoustic wavelength given by (3.6*a*). The scaling (3.6) does not therefore describe them. In the Appendix general jump conditions at a shock are given for incident linearized inviscid waves. The limiting process appropriate to the above scalings then yields the boundary condition

$$\bar{p}_1 = 0 \quad \text{at} \quad \bar{y} = \bar{y}_{\mathrm{s}}. \qquad (3.10)$$

In deriving (3.10) from the exact solution to the general linear inviscid problem, we ensure that proper account is taken of the short-wavelength entropy/vorticity waves. A multiple scales approach would be an alternative.

The entropy/vorticity waves propagate parallel to the direction of the basic flow, which is of course parallel to the wedge. It follows that in any situation where the forcing is over a distance comparable with the triple-deck scaling (3.1), i.e. over a distance which although possibly large does not extend asymptotically far upstream, the entropy/vorticity waves will be concentrated in a narrow region close to the shock. Hence they cannot affect the solution in the middle and lower decks.†

† We note that this is doubly so if $\sigma \gg Re^{-\frac{1}{38}}$ (Chapman) or $\sigma \gg Re^{-\frac{1}{37}}$ (Sutherland), since second-order viscous effects ensure that the entropy/vorticity waves decay over a distance much less than the width of the upper deck – although it follows from (2.15*d*, *e*) that the lower deck must be linear for our analysis to be valid for such values of σ.

4. The dispersion relation

Solutions to the nonlinear system (3.3), (3.4), (3.7–3.10) can in general only be obtained numerically. However, analytic solutions can be found if the waves are of small amplitude so that the system linearizes. It is then convenient to focus attention on a single mode, so we write

$$U \sim Y + h\tilde{U}\,\mathrm{e}^{\mathrm{i}(\alpha X+\beta Z-\Omega t)} + \mathrm{c.c.}, \quad (V, W, P, A) \sim h(\tilde{V}, \tilde{W}, \tilde{P}, \tilde{A})\,\mathrm{e}^{\mathrm{i}(\alpha X+\beta Z-\Omega t)} + \mathrm{c.c.}$$

Substituting into (3.3), and linearizing under the assumption that $h \ll 1$, we obtain (e.g. see Smith, Sykes & Brighton 1977)

$$\alpha\tilde{V}+\beta\tilde{W} = \frac{\mathrm{i}\beta^2\tilde{P}}{(\mathrm{i}\alpha)^{\frac{2}{3}}\,\mathrm{Ai}'(\zeta_0)}\int_{\zeta_0}^{\zeta}\mathrm{Ai}\,(q)\,\mathrm{d}q, \tag{4.1a}$$

$$\mathrm{i}^{\frac{2}{3}}\alpha^{\frac{5}{3}}\,\mathrm{Ai}'\,(\zeta_0)\,\tilde{A} = \mathrm{i}\beta^2\tilde{P}\int_{\zeta_0}^{\infty}\mathrm{Ai}\,(\zeta)\,\mathrm{d}\zeta, \tag{4.1b}$$

where

$$\zeta = (\mathrm{i}\alpha)^{\frac{1}{3}}(Y-\Omega/\alpha), \quad \zeta_0 = -\mathrm{i}^{\frac{1}{3}}\Omega/\alpha^{\frac{2}{3}}. \tag{4.2}$$

The solution to (3.7) subject to (3.8) and (3.10) is

$$\left.\begin{aligned} \tilde{\bar{p}}_1 &= \frac{\alpha^2}{(\beta^2-\alpha^2)^{\frac{1}{2}}}\frac{\sinh\left((\beta^2-\alpha^2)^{\frac{1}{2}}(\bar{y}_s-\bar{y})\right)}{\cosh\left((\beta^2-\alpha^2)^{\frac{1}{2}}\bar{y}_s\right)}\tilde{A} \quad (\beta^2 > \alpha^2),\\ \tilde{\bar{p}}_1 &= \frac{\alpha^2}{(\alpha^2-\beta^2)^{\frac{1}{2}}}\frac{\sin\left((\alpha^2-\beta^2)^{\frac{1}{2}}(\bar{y}_s-\bar{y})\right)}{\cos\left((\alpha^2-\beta^2)^{\frac{1}{2}}\bar{y}_s\right)}\tilde{A} \quad (\beta^2 < \alpha^2). \end{aligned}\right\} \tag{4.3}$$

Hence, from (4.1), (4.3) and the fact that $\tilde{P} = \tilde{\bar{p}}_1$ on $\bar{y} = 0$, it follows that

$$\frac{(\mathrm{i}\alpha)^{\frac{1}{3}}\beta^2\int_{\zeta_0}^{\infty}\mathrm{Ai}\,(\zeta)\,\mathrm{d}\zeta}{\mathrm{Ai}'\,(\zeta_0)} = \begin{cases} \dfrac{(\beta^2-\alpha^2)^{\frac{1}{2}}}{\tanh\left((\beta^2-\alpha^2)^{\frac{1}{2}}\bar{y}_s\right)} & (\beta^2 > \alpha^2)\\[2ex] \dfrac{(\alpha^2-\beta^2)^{\frac{1}{2}}}{\tan\left((\alpha^2-\beta^2)^{\frac{1}{2}}\bar{y}_s\right)} & (\beta^2 < \alpha^2). \end{cases} \tag{4.4}$$

Note that for $\beta^2 > \alpha^2$, the dispersion relation for a flow without a shock is recovered in the limit $\bar{y}_s \to \infty$ (Smith 1989).

The dispersion relation (4.4) admits both growing and decaying modes. The neutral case corresponds to

$$\zeta_0 = -c_1\,\mathrm{i}^{\frac{1}{3}}, \quad (\beta^2-\alpha^2)^{\frac{1}{2}} = c_2\,\alpha^{\frac{1}{3}}\beta^2\tanh\left((\beta^2-\alpha^2)^{\frac{1}{2}}\bar{y}_s\right), \tag{4.5}$$

where $c_1 \approx 2.3$ and $c_2 \approx 1.0$ (a similar expression exists for $\beta^2 < \alpha^2$). These are plotted as solid curves in figure 2 for three different values of $\bar{y}_s$. The diagonal dashed curve defines the wave Mach cone. Above this line the acoustic waves in the upper deck are purely sinusoidal, beneath it they either grow or decay in $\bar{y}$. When there is no shock in the upper deck, waves described by triple-deck theory are constrained to lie in the region of parameter space below the diagonal (Smith 1989); with shocks present there is no such limitation.

Asymptotic formulae for these neutral curves can be derived that agree well with the numerical results:

$$\alpha \sim \frac{(n+\frac{1}{2})\pi}{\bar{y}_s} + \left(\frac{\bar{y}_s}{2(n+\frac{1}{2})\pi} - \frac{c_2}{\bar{y}_s}\left(\frac{(n+\frac{1}{2})\pi}{\bar{y}_s}\right)^{\frac{2}{3}}\right)\beta^2, \quad \alpha = O(1), \quad \beta \ll 1, \quad n = 1, 2, \ldots, \tag{4.6a}$$

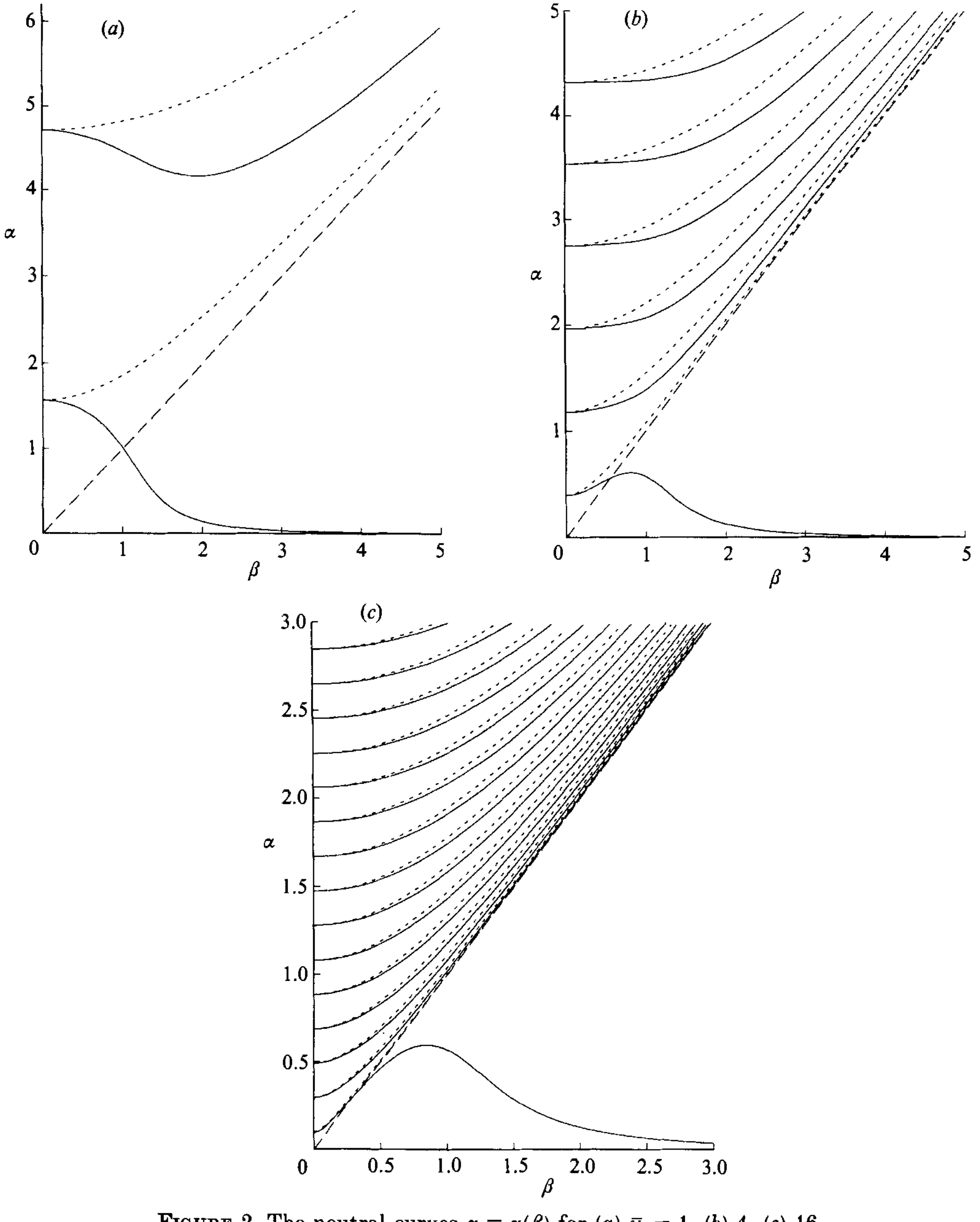

FIGURE 2. The neutral curves $\alpha \equiv \alpha(\beta)$ for (a) $\bar{y}_s = 1$, (b) 4, (c) 16.

$$\alpha \sim \beta + \left(\frac{n\pi}{\bar{y}_s}\right)^2 \frac{1}{2\beta} - \left(\frac{n\pi}{\bar{y}_s}\right)^4 \frac{1}{8\beta^3} + \frac{1}{c_2 \bar{y}_s}\left(\frac{n\pi}{\bar{y}_s}\right)^2 \frac{1}{\beta^{\frac{10}{3}}}, \quad \alpha, \beta \gg 1, \quad n = 1, 2, \ldots, \qquad (4.6b)$$

$$\alpha \sim \left(\frac{1}{c_2 \beta}\right)^3, \quad \alpha \ll 1, \beta \gg 1. \qquad (4.6c)$$

These formulae confirm that there are an infinite number of neutral waves, and that with the exception of the subsonic mode, they all asymptote to the line $\beta = \alpha$ for α, β large.

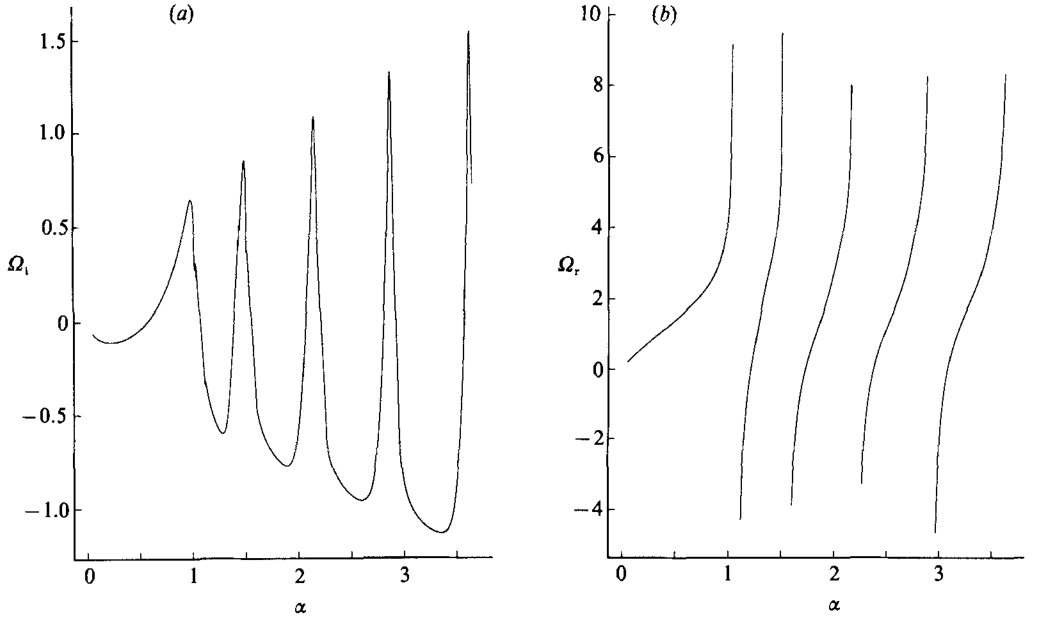

FIGURE 3. (a) The growth rate Ω_i and (b) the wave speed Ω_r as a function of α for $\bar{y}_s = 4$, $\beta = 1$.

The short-dashed lines in figure 2 also represent waves with zero growth rate, but they have an infinite frequency and hence our asymptotic analysis breaks down in their vicinity. These lines correspond to the points in the (α, β)-plane where

$$\tan\left((\alpha^2-\beta^2)^{\frac{1}{2}}\bar{y}_s\right) \to \infty.$$

More precisely if we write

$$(\alpha^2-\beta^2)^{\frac{1}{2}}\bar{y}_s = (n+\tfrac{1}{2})\pi-\delta$$

for $n = 0, 1, \ldots$, where δ is small and positive, then it follows that

$$\Omega_r = \frac{2\bar{y}_s}{\delta(2n+1)\pi}\beta^2\left[\beta^2+(n+\tfrac{1}{2})^2\frac{\pi^2}{\bar{y}_s^2}\right]^{\frac{1}{2}}+\ldots, \qquad (4.7a)$$

$$\Omega_i = \operatorname{sgn}(\delta)\left(\beta^2+(n+\tfrac{1}{2})^2\frac{\pi^2}{\bar{y}_s^2}\right)^{\frac{1}{2}}|2\Omega_r|^{-\frac{1}{2}}+\ldots. \qquad (4.7b)$$

Hence, if β is held fixed then, when α is within a distance $O(\delta)$ of a dotted curve, the disturbance has frequency $O(\delta^{-1})$ and a growth rate $O(\delta^{\frac{1}{2}})$. The wave grows or decays depending on whether it is below or above the dotted curve respectively.

It also follows from (4.7b) that the growth rates in the unstable regions above $\alpha = \beta$ increase with n. In fact if we hold β fixed and let $\alpha \to \infty$, analysis of (4.4) shows that the unstable intervals are of range $O(\alpha^{-\frac{2}{3}})$ and that the growth rates in the unstable intervals are typically $O(\alpha^{\frac{2}{3}})$. The frequency in the unstable intervals also increases like $\alpha^{\frac{2}{3}}$, and so the unstable intervals for $n \gg 1$ correspond to high-frequency, short-wavelength modes with increasingly high growth rates. However, the fact that these modes occur over decreasingly short ranges in α as n is increased means that they might not be excited naturally in a physically realistic flow situation.

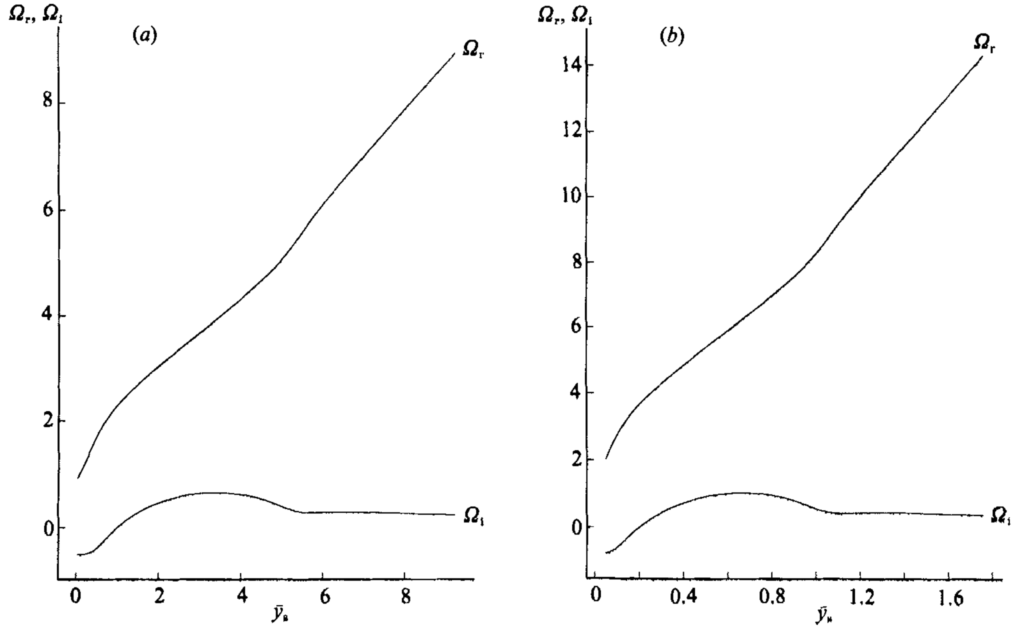

FIGURE 4. Ω_r and Ω_i as functions of $\bar{y}_s$ for (a) $\beta = 1$, $\alpha = 0.999\beta$; (b) $\beta = 2$, $\alpha = 0.999\beta$.

In figure 3 we show the dependence of Ω_r and Ω_i on α for the case $\bar{y}_s = 4$, $\beta = 1$. We observe the predicted monotonic increase in the growth rates and the shortening of the range of unstable wavenumbers as α increases. Results at other values of $\bar{y}_s$ and β are similar, with the range over which the oscillations in α occur decreasing as either $\bar{y}_s$ or β is increased.

It is perhaps significant that the modes which reduce to those discussed by Smith (1989) when $\bar{y}_s \rightarrow \infty$, i.e. the subsonic modes, have growth rates less than those with $\beta < \alpha$. As a measure of the growth rate of the subsonic mode we can take its value close to the line $\alpha = \beta$. In fact in all the cases calculated we found that this mode had its maximum value in this neighbourhood. In figure 4, we show the dependence of Ω_i on $\bar{y}_s$ for different values of the spanwise wavenumber β with $\alpha = 0.999\beta$. We see that Ω_i increases to a maximum and then decreases. Thus, for a given (α, β) close to the line $\beta = \alpha$ there is an optimum value of $\bar{y}_s$ which maximizes the growth rate. In fact it follows from (4.4) that if

$$\alpha^2 - \beta^2 = \Delta \quad \text{with} \quad |\Delta| \ll 1, \quad \bar{y}_s |\Delta|^{\frac{1}{3}} \ll 1,$$

then, close to $\alpha = \beta$,

$$\bar{y}_s \, \mathrm{i}^{\frac{1}{3}} \alpha^{\frac{7}{3}} \approx \frac{\mathrm{Ai}'(\zeta_0)}{\int_{\zeta_0}^{\infty} \mathrm{Ai}(\zeta)\, \mathrm{d}\zeta}.$$

Asymptotic analysis for this expression for small and large $\bar{y}_s$ demonstrates that the growth rate has a maximum for intermediate $\bar{y}_s$, e.g.

$$\Omega \sim \alpha^3 \bar{y}_s + \left(\frac{\mathrm{i}}{\alpha \bar{y}_s}\right)^{\frac{1}{2}} \quad \text{as} \quad \bar{y}_s \rightarrow \infty.$$

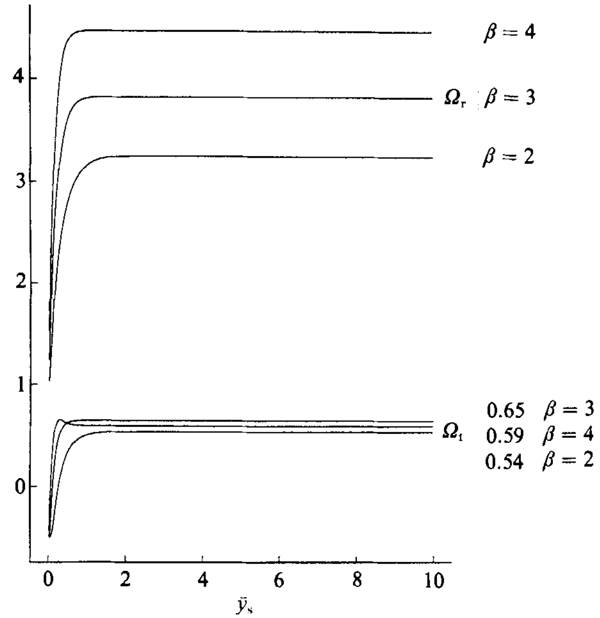

FIGURE 5. The growth rates and phase speeds as a function of $\bar{y}_s$ for $\alpha = 1$, $\beta = 2, 3, 4$.

We note however that if $\bar{y}_s|\Delta|^{\frac{1}{2}}$ is not small then the above simplification does not hold. Further for $\bar{y}_s|\Delta|^{\frac{1}{2}}$ large the asymptotic behaviour depends on the sign of Δ. If $\Delta < 0$, then the eigenrelation (4.4) reduces to

$$(\mathrm{i}\alpha)^{\frac{1}{3}}\beta^2 \int_{\zeta_0}^{\infty} \mathrm{Ai}\,(\zeta)\,\mathrm{d}\zeta = (\beta^2-\alpha^2)^{\frac{1}{2}}\,\mathrm{Ai}'\,(\zeta_0), \tag{4.8}$$

which is valid for $\bar{y}_s \gg 1$, α, $\beta = O(1)$. As expected this is the eigenrelation of Smith (1989). In figure 5 we show the dependence of Ω_r and Ω_i on $\bar{y}_s$ for different values of β with $\alpha = 1$. For these subsonic modes the growth rates approach constant values as $\bar{y}_s \to \infty$, in agreement with Smith's (1989) shock-free analysis. Hence subsonic modes of fixed wavelength do not feel the presence of the shock when $\bar{y}_s$ is large (nor do short-wavelength subsonic modes when $\bar{y}_s = O(1)$). However, if $\bar{y}_s \to \infty$ with $\Delta > 0$ there is no simplification similar to (4.8) since the growth rate oscillates, with the regions of stability and instability becoming increasingly thin as $\bar{y}_s$ is increased.

As indicated above, the structure of the eigenfunctions associated with the different modes shown in figure 2 depends on the sign of Δ. If $\beta > \alpha$ then the disturbances are described by a combination of exponentially growing and decaying functions. In any of the limits where the shockless eigenrelation is recovered, e.g. $\bar{y}_s \to \infty$ or $\beta \to \infty$, the exponentially decaying function dominates and the eigenfunctions also tend to those of the shockless problem. The modes which have $\beta < \alpha$ are described by trigonometric functions and therefore in any limit involving $\bar{y}_s$, β_1 or α they are oscillatory and $O(1)$ between the wedge and the shock. This class of the mode is perhaps best thought of as sound waves trapped between the wedge and shock and amplified by the boundary layer.

5. The inviscid modes

So far we have only discussed the effect of the shock on viscous modes of instability yet it is well-known that compressible shear flows can also support unstable inviscid disturbances. The inviscid modes of instability for a compressible boundary layer have wavelengths comparable with the boundary-layer thickness so we consider perturbations to the flow described in §2 but with wavelengths scaled on the main-deck thickness. In order to be consistent with previous investigations we drop the rescaling (3.1) introduced in order to simplify the triple-deck analysis of §3. We also relax the Newtonian assumption (2.11), allow for a non-unity Prandtl number, and assume Chapman's viscosity law (see Blackaby & Hall 1989 for the changes necessary when Sutherland's law is used).

Following for example Mack (1987), we scale wavelengths on the main-deck thickness and the wave speed on the free-stream speed. The pressure perturbation P for an inviscid mode then satisfies the compressible Rayleigh equation

$$P''-\frac{2\bar{u}'}{\bar{u}-c}P'+\frac{\bar{T}'}{\bar{T}}P'-(\alpha^2+\beta^2)\left(1-\frac{\alpha^2(\bar{u}-c)^2M^2}{(\alpha^2+\beta^2)\,\bar{T}}\right)P=0. \tag{5.1}$$

Here a prime denotes a derivative with respect to boundary-layer variable y^*, whilst the basic velocity field $\bar{u}$ and temperature $\bar{T}$ for an insulated wall are given by

$$\bar{u}=f'(\eta),\quad \bar{T}=1+Pr(\gamma-1)M^2\int_0^{\infty}(f''(q))^{Pr}\,\mathrm{d}q\int_0^{q}(f''(p))^{2-Pr}\,\mathrm{d}p, \tag{5.2a, b}$$

where f is the Blasius function and η is the Dorodnitsyn–Howarth variable defined by

$$\eta=\frac{1}{(2C)^{\frac{1}{2}}}\int_0^{y^*}\frac{\mathrm{d}y^*}{\bar{T}}. \tag{5.2c}$$

The quantities $\alpha/(2C)^{\frac{1}{2}}$ and $\beta(2C)^{\frac{1}{2}}$ are downstream and spanwise wavenumbers, whilst c is the wave speed. In terms of the Dorodnitsyn–Howarth variable, the Rayleigh equation (5.1) becomes

$$\frac{\mathrm{d}^2P}{\mathrm{d}\eta^2}-\frac{2f''}{f'-c}\frac{\mathrm{d}P}{\mathrm{d}\eta}-(\alpha^2+\beta^2)\,\bar{T}\left(\bar{T}-\frac{\alpha^2(f'-c)^2M^2}{(\alpha^2+\beta^2)}\right)P=0. \tag{5.2d}$$

We confine our attention to modes that satisfy

$$P'=0\quad\text{on}\quad\eta=0,\quad P\rightarrow 0\quad\text{as}\quad\eta\rightarrow\infty, \tag{5.3a, b}$$

which together with (5.2d) specify an eigenrelation $c=c(\alpha,\beta)$. One of the points at issue here is whether the decay of P when $\eta\rightarrow\infty$ is sufficiently rapid to mean that the shock located outside the boundary layer has a negligible effect on the disturbance. In order to see whether this is the case we discuss the structure of solutions of (5.2d) in the limit $M\rightarrow\infty$.

Since this work was completed we learned of an independent investigation of (5.1) for $M\gg 1$ by S. N. Brown and F. T. Smith. *Inter alia* they have concentrated on the so-called vorticity mode (Mack 1987), while we shall study the acoustic modes. We restrict our discussion of (5.2d) to the minimum that explains the large M structure of P and shows that in the wedge problem considered in this paper the shock generally has only an exponentially small effect on the eigenrelation except for wedges of thickness comparable to the boundary layer. Further, we concentrate on the generalized inflection point neutral modes of (5.2*d*) which have $\beta = 0$. The discussion we give can be extended to unstable two- and three-dimensional modes, although as indicated below an extra critical-layer region then needs to be included.

The generalized inflection point occurs where $\bar{u}_{y_* y_*}\bar{T} = \bar{u}_{y_*}\bar{T}_{y_*}$, and if we write

$$\eta = B + [2\log M^2]^{\frac{1}{2}} - \frac{\log[2\log M^2]^{\frac{1}{2}} + \log\tilde{Y}}{[2\log M^2]^{\frac{1}{2}}}, \tag{5.4}$$

where the constant B comes from the large-η asymptotic form of f:

$$f = \eta - B + \frac{d\,\mathrm{e}^{-(\eta-B)^2/2}}{(\eta-B)^2} + \ldots, \tag{5.5a}$$

then we can show that it occurs at

$$\tilde{Y} = \tilde{Y}_c = \frac{1}{(\gamma-1)\,d},$$

where d is another known constant. The wave speed is then given by $\bar{u}$ evaluated at the inflection point so that (5.2*d*) is not singular there. Thus, we have

$$c = 1 - \frac{\tilde{c}_1}{M^2} + \ldots, \tag{5.5b}$$

with $\tilde{c}_1 = 1/(\gamma-1)$.

Next we anticipate the change of scale of the boundary layer for $M \gg 1$ and write

$$\alpha = \frac{A_0}{M^2} + \ldots.$$

It follows that the zeroth-order approximation to (5.2*d*) for $O(1)$ values of η is

$$\frac{\mathrm{d}^2 P_0}{\mathrm{d}\eta^2} - \frac{2f''}{f'-1}\frac{\mathrm{d}P_0}{\mathrm{d}\eta} - \frac{A_0^2(\gamma-1)^2(1-f'^2)^2}{4}\left(1 - \frac{2(1-f')}{(\gamma-1)(1+f')}\right)P_0 = 0. \tag{5.6}$$

For large values of η it is found that the solutions of (5.6) are such that

$$P_0 \sim \frac{D_0\,\mathrm{e}^{-(\eta-B)^2}}{(\eta-B)^3} + E_0, \tag{5.7a}$$

where D_0 and E_0 are arbitrary constants. One of these constants can be fixed as a normalization condition, while the other is then determined by investigating the solution of (5.2*d*) in the region where $\tilde{Y} = O(1)$, and also in the region above this logarithmically thin layer. In passing it is of interest to note that this layer also controls the Görtler vortex mechanism in hypersonic boundary layers (Hall & Fu 1989).

In seeking an asymptotic expansion for $\tilde{Y} = O(1)$, we note from (5.2*d*) that for $1 \ll \eta \ll M^2$, the leading-order approximation for P can be written as

$$P \sim E - \frac{2D}{d^2}\int_{\eta_c}^{\eta} (f'-c)^2\,\mathrm{d}\eta, \tag{5.7b}$$

where η_c is the position of the generalized inflection point. The leading term for $\tilde{Y} = O(1)$ can be found by direct expansion of this expression. Alternatively, with

$$P = \tilde{P}_0(\tilde{Y}) + \ldots, \tag{5.8a}$$

we find after some manipulation that $\tilde{P}_0$ satisfies

$$\tilde{Y}^2\frac{\mathrm{d}^2\tilde{P}_0}{\mathrm{d}\tilde{Y}^2}+\tilde{Y}\frac{\mathrm{d}\tilde{P}_0}{\mathrm{d}\tilde{Y}}+\frac{2\,\mathrm{d}\tilde{Y}^2}{\tilde{c}_1-\mathrm{d}\tilde{Y}}\frac{\mathrm{d}\tilde{P}_0}{\mathrm{d}\tilde{Y}}=0, \tag{5.8b}$$

which is to be solved in the range $0<\tilde{Y}<\infty$. The solution of this equation is

$$\tilde{P}_0=\tilde{D}_0(\tfrac{1}{2}d^2\tilde{Y}^2-2\tilde{c}_1 d\tilde{Y}+\tilde{c}_1^2\log\tilde{Y})+\tilde{E}_0, \tag{5.8c}$$

where $\tilde{D}_0$ and $\tilde{E}_0$ are constants. This solution is to be matched with (5.7) when $\tilde{Y}\rightarrow\infty$ so that

$$\tilde{D}_0=\frac{2D_0}{d^2M^4(2\log M^2)^{\frac{1}{2}}}+\ldots.$$

Above this logarithmically thin region there is an outer region with the scaled coordinate $\bar{\eta}=M^{-2}\eta$ (note from (5.2c) that $y^*=O(1)$ in this region). The solution there is

$$P=\bar{E}_0\exp\left[-\alpha(1-(1-c)^2M^2)^{\frac{1}{2}}\eta\right]+O(\exp)\sim\bar{E}_0\exp(-A_0\bar{\eta}).$$

Matching this solution to the logarithmic term in (5.8c) for $\tilde{Y}$ small we find that

$$\bar{E}_0\sim\frac{2\tilde{c}_1^2D_0}{A_0d^2M^2},$$

and matching to the constant yields

$$\tilde{E}_0\sim\bar{E}_0.$$

Note that this means that the constant term dominates the $\tilde{Y}$-dependent part of the complementary function in (5.8c). However, on substituting (5.8c) into (5.2c) we confirm that (5.8b) is still the leading-order equation for $\tilde{P}_0'(\tilde{Y})$. An alternative way to see this is to work with the equation for the velocity fluctuation normal to the wall, rather than that for the pressure fluctuation.

Finally, matching back to the lower layer adjacent to the wall we conclude that

$$E_0\sim\tilde{E}_0\sim\bar{E}_0\ll 1.$$

Therefore, A_0 is determined by the eigenvalue problem specified by (5.6) together with

$$P_0'=0\quad\text{on}\quad\eta=0,\quad P_0\rightarrow 0\quad\text{as}\quad\eta\rightarrow\infty. \tag{5.9}$$

This problem was solved numerically with $\gamma=1.4$ and $Pr=1$ to yield the sequence of eigenvalues $A=4.81$, 13.84, 23.34, 33.03, 42.82, 52.67, 62.55, 72.45, 82.37, 92.29, ... In figure 6(*a*) we have plotted our one-term asymptotic prediction of α together with the values which we obtained by a full numerical solution of the inviscid stability equation (5.2*d*). This was done by deforming the path of integration into the complex plane in order to avoid difficulties near the generalized inflection point. We are grateful to P. W. Duck for comments on the efficient solution of the full inviscid equation. The comparison made in figure 6(*a*) shows that the hypersonic prediction we have made agrees well with the solution of the full problem over a wide range of Mach numbers. Surprisingly the agreement between the curves is better for the lower inviscid modes; we have no explanation of why this should be the case. The eigenfunctions associated with the above set of eigenvalues are illustrated in figure 7.

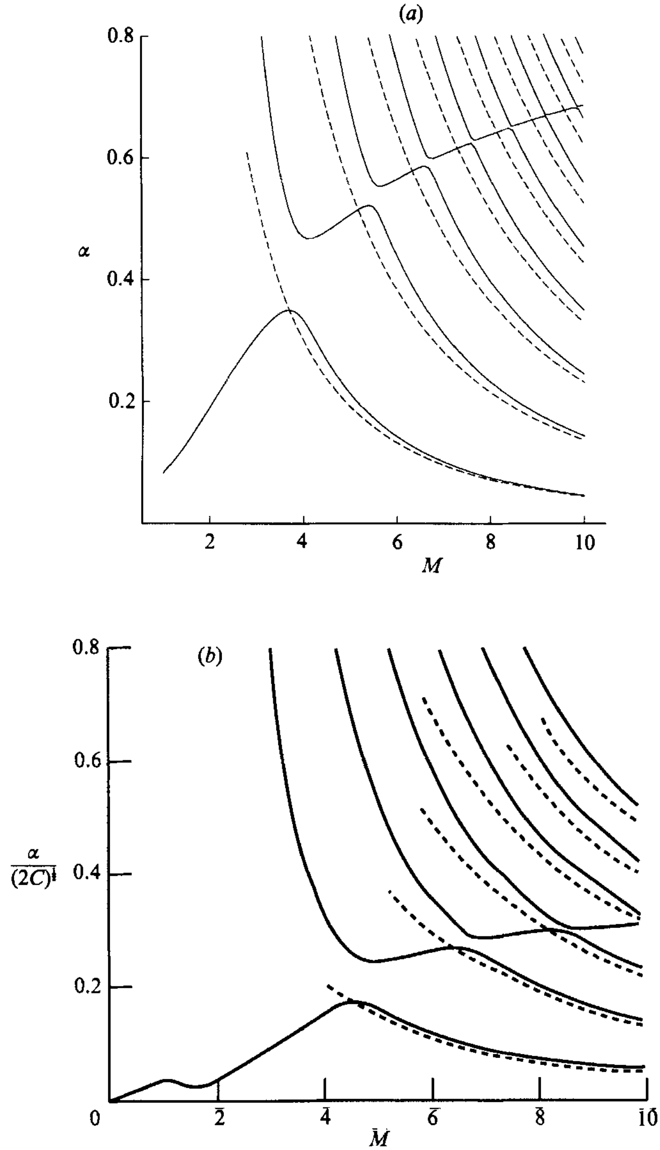

FIGURE 6. (*a*). The neutral curves predicted by the asymptotic theory for large M (----) and the numerical solution of (5.2*d*) (——); $\gamma = 1.4$, $Pr = 1$, $\beta = 0$. (*b*) The neutral curves for the generalized inflection point modes. Mack's (1987) results (——) and the high-M asymptotic prediction (----); $\gamma = 1.4$, $Pr = 0.71$, $\beta = 0$.

We now turn to a comparison of our results with those of Mack (1987). A direct comparison is difficult because Mack apparently used a combination of Chapman's and Sutherland's laws to describe the viscosity–temperature dependence. The theory presented here is not valid for Sutherland's law (see Blackaby & Hall 1989), but in order to compare with Mack we use Chapman's law and evaluate the Chapman constant by making the law exactly correct at the wall. The wall and free-stream viscosities in the resulting definition of C are then evaluated using Sutherland's law; a consequence of this well-known approximation is that C then effectively becomes a function of the Mach number for a given set of wall and free-stream temperature conditions. In this way we can obtain results that can be compared with Mack's; however a further minor alteration is that the Prandtl number must be changed from unity to the value 0.71 appropriate for air. For this new Prandtl number the set of eigenvalues is $A = 5.07, 14.33, 24.07, 34.02, 44.08, 54.20, 64.35, 74.52, 84.71, 94.91, \ldots$. Thus the eigenvalues vary little when the Prandtl number is changed. In order to bring in the effect of the Chapman constant, and be consistent with Mack's scaling, these values must be rescaled by dividing by $(2C)^{\frac{1}{2}}$. In figure 6(*b*) we have compared our results with Mack's over a range of Mach numbers; as for the previous case we have good agreement between the different methods, at least for the lower modes. Finally, we note that the higher-order modes of the eigenvalue problem can be derived by applying the WKB method to (5.6). In fact we anticipate that the WKB description of the modes discussed above, coupled to the vorticity mode description of S. N. Brown & F. T. Smith mentioned earlier in this section, could be used to explain the kinks in the neutral curves given by Mack. Thus we expect that these eigenvalues are split apart by an exponentially small amount in the manner discussed by, for example, DiPrima & Hall (1984) for the Taylor problem.

With the structure of the neutral mode thus identified, the form of the unstable modes can be determined. Suppose that

$$c = 1 - \frac{\tilde{c}_1}{M^2} + \ldots + \frac{\tilde{c}_i}{M^4(2\log M^2)^{\frac{1}{2}}} + \ldots, \tag{5.10a}$$

where $\tilde{c}_i$ is the leading-order complex term, and $\tilde{c}_1$ is not necessarily equal to $1/(\gamma-1)$, cf. (5.5*b*). Then for $\tilde{Y} = O(1)$, (5.8*a*) is generalized to

$$\begin{aligned} P = {} & \frac{2\tilde{c}_1^2 D_0}{A_0 d^2 M^2}\left(1 + \ldots + \frac{E_i}{M^2(2\log M^2)^{\frac{1}{2}}} + \ldots\right) \\ & + \frac{2D_0}{d^2 M^4 (2\log M^2)^{\frac{1}{2}}}\left(1 + \ldots + \frac{D_i}{M^2(2\log M^2)^{\frac{1}{2}}} + \ldots\right)(\tfrac{1}{2}d^2\tilde{Y}^2 - 2\tilde{c}_1 d\tilde{Y} + \tilde{c}_1^2 \log\tilde{Y}) + \ldots \\ & + \frac{1}{M^6(2\log M^2)}\tilde{P}_i + \ldots, \end{aligned} \tag{5.10b}$$

where the first two terms represent the asymptotic expansions of (5.7*b*), E_i and D_i are the leading-order complex terms (D_0 is taken to be real), and $\tilde{P}_i$ satisfies

$$\tilde{Y}^2 \frac{d^2\tilde{P}_i}{d\tilde{Y}^2} + \tilde{Y}\frac{d\tilde{P}_i}{d\tilde{Y}} + \frac{2\,d\tilde{Y}^2}{\tilde{c}_1 - d\tilde{Y}}\frac{d\tilde{P}_i}{d\tilde{Y}} = \frac{2A_0 D_0 \tilde{c}_1^2}{d^2}(1 + (\gamma-1)\,d\tilde{Y})^2 - \frac{4D_0 \tilde{c}_i \tilde{Y}}{d}. \tag{5.11a}$$

Hence

$$\begin{aligned} \tilde{Y}\tilde{P}_{i\tilde{Y}} \sim {} & \frac{2A_0 D_0}{d^2}(\tilde{c}_1 - d\tilde{Y})^2\left(\log\tilde{Y} + ((\gamma-1)^2\tilde{c}_1^2 - 1)\log|\tilde{c}_1 - d\tilde{Y}| + \frac{\tilde{c}_1(1+\tilde{c}_1(\gamma-1))^2}{\tilde{c}_1 - d\tilde{Y}}\right) \\ & + \frac{4D_0\tilde{c}_i(d\tilde{Y} - \tilde{c}_1)}{d^2}. \end{aligned} \tag{5.11b}$$

If $\tilde{c}_1 \neq 1/(\gamma-1)$, then there must be a jump in D_i across the critical layer $\tilde{Y} = \tilde{c}_1/d$. Further, from matching with the solution for $\eta = O(1)$, D_i can be assumed to be real for $\tilde{Y} > \tilde{c}_1/d$; hence for $\tilde{Y} < \tilde{c}_1/d$ and $\mathrm{Im}(\tilde{c}_i) > 0$, it follows from a standard linear critical-layer analysis that

$$\mathrm{Im}(D_i) = \pi A_0((\gamma-1)^2\tilde{c}_1^2 - 1). \tag{5.12a}$$

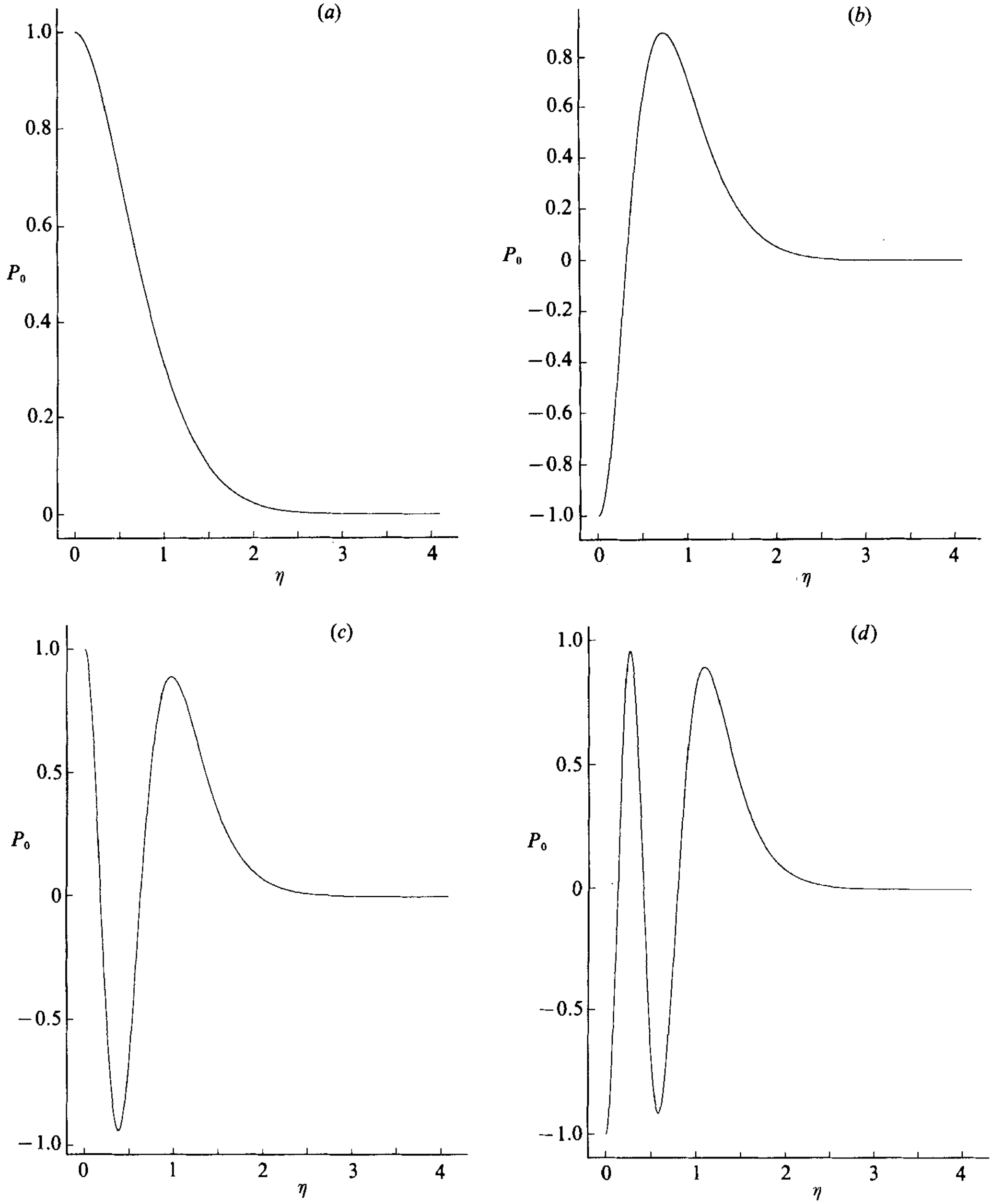

FIGURE 7 (*a–d*). For caption see facing page.

Matching with the solution where $\bar{\eta} = O(1)$, implies that

$$\operatorname{Im}(E_i) = \operatorname{Im}\left(D_i - \frac{2\tilde{c}_i}{\tilde{c}_1}\right). \tag{5.12b}$$

$\operatorname{Im}(\tilde{c}_i)$ can now be fixed by looking at higher-order terms in the solution for $\eta = O(1)$. Let

$$P = P_0 + \ldots + \frac{D_0}{M^4(2\log M^2)^{\frac{1}{2}}} P_i + \ldots, \tag{5.13a}$$

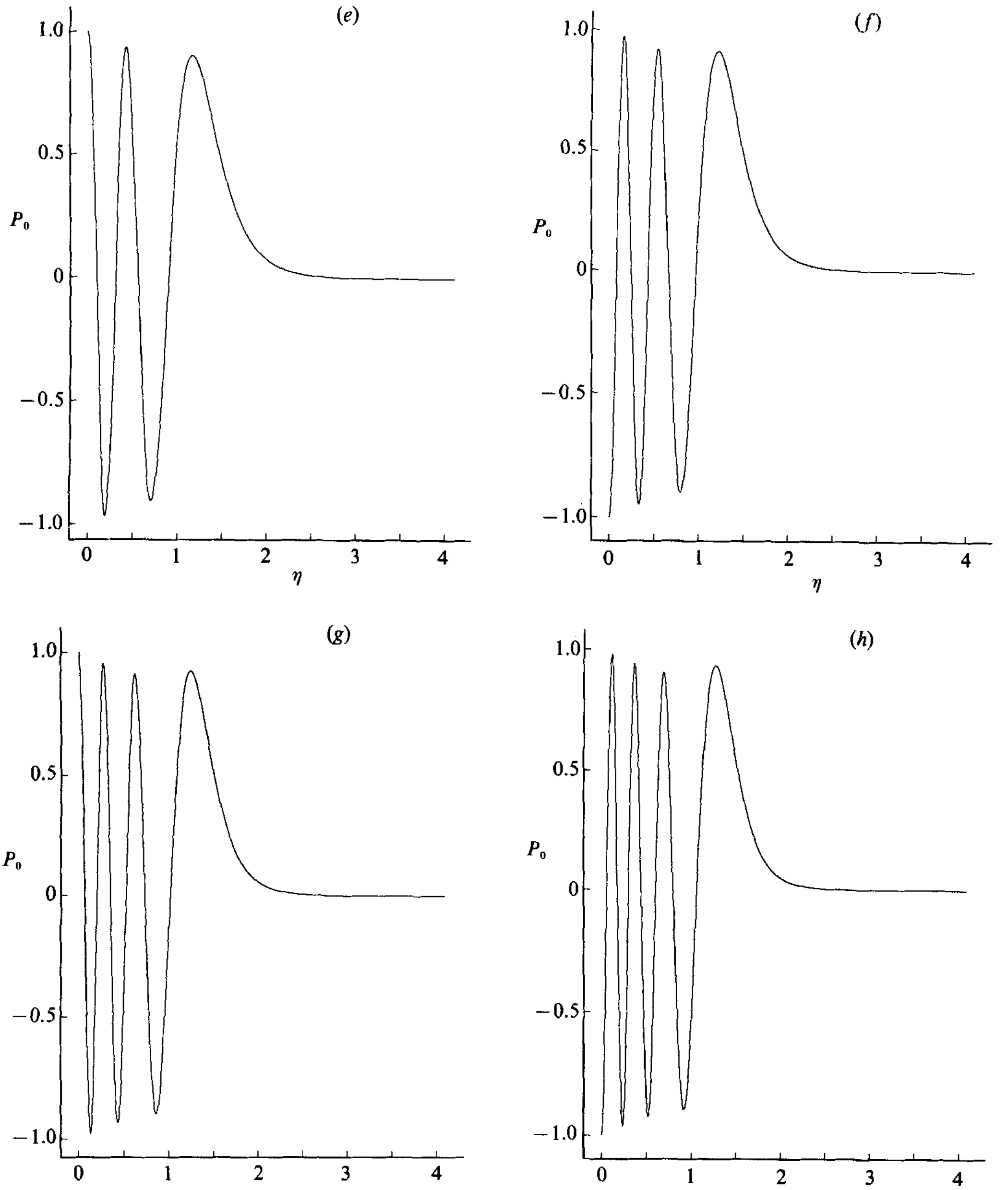

FIGURE 7. (*a*) The eigenfunction $P_0(y)$ for (*a*) $A = 4.81$, (*b*) 13.84, (*c*) 23.34, (*d*) 33.03, (*e*) 42.82, (*f*) 52.67, (*g*) 62.55, (*h*) 72.45. $\gamma = 1.4$, $Pr = 1$.

then the governing equation for $\operatorname{Im}(P_i)$ is

$$\operatorname{Im}\left(\frac{\mathrm{d}^2 P_i}{\mathrm{d}\eta^2}-\frac{2f''}{f'-1}\frac{\mathrm{d}P_i}{\mathrm{d}\eta}-\frac{A_0^2(\gamma-1)^2(1-f'^2)^2}{4}\left(1-\frac{2(1-f')}{(\gamma-1)(1+f')}\right)P_i\right)$$
$$=\frac{\operatorname{Im}(\tilde{c}_i)}{D_0}\left(\frac{2f''}{(f'-1)^2}\frac{\mathrm{d}P_0}{\mathrm{d}\eta}+A_0^2(\gamma-1)(1-f'^2)(f'-1)P_0\right), \quad (5.13b)$$

subject to $P_i' = 0$ on $\eta = 0$. The existence of the eigensolution P_0 implies that we can take $P_i = 0$ on $\eta = 0$ without loss of generality, and we suppose that the numerical solution to (5.13*b*) yields

$$\operatorname{Im}(P_i) \rightarrow \operatorname{Im}(\tilde{c}_i)K \quad \text{as} \quad \eta \rightarrow \infty, \tag{5.13c}$$

where K is a numerically determined real constant. Then the matching condition with (5.10*b*) yields

$$\operatorname{Im}(\tilde{c}_i)K \rightarrow \frac{2\pi\tilde{c}_1^2}{d^2}((\gamma-1)^2\tilde{c}_1^2-1) - \frac{4\tilde{c}_1 \operatorname{Im}(\tilde{c}_i)}{A_0 d^2} \quad \text{as} \quad \eta \rightarrow \infty. \tag{5.13d}$$

Since we have assumed that $\operatorname{Im}(\tilde{c}_i) > 0$, this eigenproblem for $\operatorname{Im}(\tilde{c}_i)$ can only be satisfied for one sign of $(1-(\gamma-1)^2\tilde{c}_1^2)$. On the basis of Mack's (1987) solutions of (5.1), we anticipate that the growing modes can be found for $0 < \tilde{c}_1 < 1/(\gamma-1)$, where the lower bound is necessary if there is to be a critical layer at all. Hence

$$\operatorname{Im}(\tilde{c}_i) = \frac{2\pi A_0 \tilde{c}_1^2((\gamma-1)^2\tilde{c}_1^2-1)}{(KA_0 d^2 + 4\tilde{c}_1)} \quad \text{for} \quad 0 < \tilde{c}_1 < \frac{1}{\gamma-1}. \tag{5.14}$$

6. Conclusions

We have shown that if shock effects are to be included in a Tollmien–Schlichting stability analysis of flow past a wedge, then the Newtonian approximation, $(\gamma-1) \ll 1$, must be made if the complicating effects of non-parallelism are to be avoided. With this assumption we have seen that the viscous modes have their dispersion relationship crucially altered by the presence of a shock at a distance $\bar{y}_s$ from the wedge scaled on the upper-deck thickness. In the limit $\bar{y}_s \rightarrow \infty$ Smith's (1989) mode is recovered, and the shock has no zeroth-order effect on the mode's growth rate. In addition to this mode, there is an infinite discrete spectrum of disturbances which persist to the shock. These modes have large growth rates at high frequencies, but occur only over small ranges of wavenumber, which suggests that the frequency might have to be tuned to produce instability. It is therefore an open question as to whether these additional modes play a critical role in the transition process in hypersonic flows. We also point out that where our analysis predicts infinite frequencies, i.e. close to the short-dashed curves in figure 2(*a–c*), then our asymptotic expansions fails and a new structure must be set up in order to account for the faster disturbance response. This problem has not been investigated in this paper.

The main result of the inviscid mode analysis is that the high-Mach-number structure of the inviscid modes does not lead to a reduced rate of decay at infinity. Hence the shock cannot have a direct effect on these modes, at least until its distance from the wall is comparable with the thickness of the boundary layer. Then the steady flow changes and the effect of the shock may be felt within the outer region. As S. N. Brown & F. T. Smith (private communication) have shown, the vorticity mode is concentrated in the logarithmically small region specified by the scaling (5.4). Outside this region the mode decays rapidly; as a result the shock has no direct effect on the structure of the vorticity mode, other than by changing the mean velocity profile through shock-wave heating (Lees 1956; Blackaby, Cowley & Hall 1989).

The authors are grateful to T. Zang for directing our attention to the entropy and shear waves, and to G. Erlebacher, M. Y. Hussaini and P. W. Duck for discussions. They also thank a referee for pointing out that our initial comparison with Mack's (1987) results was made under false assumptions. This research was supported by the National Aeronautics and Space Administration under Contract No. NAS1-18107 while the authors were in residence at the Institute for Computer Applications in Science and Engineering (ICASE), NASA Langley Research Center, Hampton, VA 23665.

Appendix. Shock conditions

In this Appendix we give the conditions that must hold at the shock – see Moore (1954), Ribner (1954) and McKenzie & Westphal (1968) for similar derivations.

For convenience we now work with the coordinates (ξ, η, z) defined in (2.7). We also redefine (u, v, w) to be the velocities parallel to the shock, normal to the shock, and in the spanwise direction, respectively. Therefore, for a shock given by $\eta = f(\xi, z, t)$, the jump conditions across the shock are (e.g. Majda 1983)

$$\left.\begin{aligned}
&\frac{\partial f}{\partial t}[p]+\frac{\partial f}{\partial \xi}[\rho u]-[\rho v]+\frac{\partial f}{\partial z}[\rho w] = 0,\\
&\frac{\partial f}{\partial t}[\rho u]+\frac{\partial f}{\partial \xi}[\rho u^2+p]-[\rho uv]+\frac{\partial f}{\partial z}[\rho uw] = 0,\\
&\frac{\partial f}{\partial t}[\rho v]+\frac{\partial f}{\partial \xi}[\rho uv]-[\rho v^2+p]+\frac{\partial f}{\partial z}[\rho vw] = 0,\\
&\frac{\partial f}{\partial t}[\rho w]+\frac{\partial f}{\partial \xi}[\rho uw]-[\rho vw]+\frac{\partial f}{\partial z}[\rho w^2+p] = 0,\\
&\frac{\partial f}{\partial t}[\rho \mathscr{E}]+\frac{\partial f}{\partial \xi}[u(\rho \mathscr{E}+p)]-[v(\rho \mathscr{E}+p)]+\frac{\partial f}{\partial z}[w(\rho \mathscr{E}+p)] = 0,
\end{aligned}\right\} \qquad (\mathrm{A}\,1)$$

where $\mathscr{E} = p/[(\gamma-1)\rho]+\frac{1}{2}(u^2+v^2+w^2)$. The basic solution specified by (2.2) can be shown to satisfy these jump conditions with $f \equiv 0$.

We assume that there is a small disturbance beneath the shock and write

$$(\rho, u, v, w, p, \mathscr{E}) = (R, U, V, W, P, E)+(\tilde{r}, \tilde{u}, \tilde{v}, \tilde{w}, \tilde{p}, \tilde{e}). \qquad (\mathrm{A}\,2a)$$

For our flow any waves above the shock propagate towards the shock. Hence the disturbance cannot extend above the shock, where we write

$$(\rho, u, v, w, p, \mathscr{E}) = (\bar{R}, \bar{U}, \bar{V}, \bar{W}, \bar{P}, \bar{E}). \qquad (\mathrm{A}\,2b)$$

The linearized shock conditions are obtained by substituting (A 2) into (A 1) and neglecting all nonlinear disturbance terms. The position of the shock will vary by only a small amount from $\eta = 0$, so we write $f = \tilde{f}$. Also, since the undisturbed flow is a constant above and below the shock, to a consistent approximation the jump conditions can be evaluated at $\eta = 0$ instead of $\eta = \tilde{f}$. Finally, we assume that the linear disturbance can be expressed as a superposition of Fourier modes, so that it is sufficient to study a single mode, i.e. we assume

$$\tilde{\rho} \propto \exp(\mathrm{i}(\alpha\xi+\beta z-\Omega t)), \text{etc.} \qquad (\mathrm{A}\,3)$$

Note that here α, β and Ω are not the scaled quantities of §4. After a little manipulation it follows from (A 1) that

$$\left.\begin{aligned} -\mathrm{i}(\Omega-\alpha U)(\bar{R}-R)\tilde{f}+R\tilde{v}+V\tilde{r}=0, \quad \mathrm{i}\alpha(\bar{P}-P)\tilde{f}+RV\tilde{u}=0, \\ 2RV\tilde{v}+V^2\tilde{r}+\tilde{p}=0, \quad RV\tilde{w}+\mathrm{i}\beta(\bar{P}-P)\tilde{f}=0, \\ -\mathrm{i}(\Omega-\alpha U)(\overline{RE}-RE)\tilde{f}+\mathrm{i}\alpha U(\bar{P}-P)\tilde{f}+(RE+P)\tilde{v}+VR\tilde{e}+VE\tilde{r}+V\tilde{p}=0. \end{aligned}\right\} \quad (\mathrm{A}\ 4)$$

$\tilde{f}$ and $\tilde{r}$ can be eliminated from the above to obtain

$$\left.\begin{aligned} \beta\tilde{u}-\alpha\tilde{w}=0, \quad RV\tilde{v}+\tilde{p}-\frac{(\Omega-\alpha U)RV}{\alpha\bar{V}}\tilde{u}=0, \\ \left[\frac{\gamma}{\gamma-1}P+\tfrac{1}{2}R(V^2-U^2)\right]\tilde{v}+\left[\frac{\gamma+1}{2(\gamma-1)}V-\frac{U^2}{2V}\right]\tilde{p}+\frac{(\Omega-\alpha V)(\overline{RE}-RE)RV}{\alpha(\bar{P}-P)}\tilde{u}=0, \end{aligned}\right\} \quad (\mathrm{A}\ 5)$$

where for our basic state and non-dimensionalization

$$R=1, \quad P=\frac{1}{\gamma M^2}, \quad U=\frac{1}{(1+\epsilon^2\mathscr{T}^2)^{\frac{1}{2}}}, \quad V=\epsilon\bar{V}, \quad \bar{V}=-\frac{\mathscr{T}}{(1+\epsilon^2\mathscr{T}^2)^{\frac{1}{2}}},$$

$$\bar{P}=\frac{\epsilon}{\gamma M^2}-\frac{\epsilon(\gamma-1)(1-\epsilon^2)\mathscr{T}^2}{2\gamma(1+\epsilon^2\mathscr{T}^2)}, \quad \mathscr{T}=\tan\sigma.$$

Beneath the shock the linear waves have solutions proportional to $\mathrm{e}^{\mathrm{i}\boldsymbol{k}\cdot\boldsymbol{\xi}-\mathrm{i}\Omega t}$, where $\boldsymbol{k}=(\alpha,\nu,\beta)$ and $\boldsymbol{\xi}=(\xi,\eta,z)$. The solutions for the different types of wave satisfy the linearized inviscid Euler equations, and have the following forms:
acoustic:

$$\left.\begin{aligned} (\Omega-\boldsymbol{U}\cdot\boldsymbol{k})^2=k^2a^2 \quad \text{where} \quad \boldsymbol{U}=(U,V,0), \quad a^2=\frac{\gamma P}{R}, \\ (\tilde{p},\tilde{r})=\left(1,\frac{1}{a}\right)\mathrm{e}^{\mathrm{i}\boldsymbol{k}\cdot\boldsymbol{\xi}-\mathrm{i}\omega t}, \quad (\tilde{u},\tilde{v},\tilde{w})=\frac{\boldsymbol{k}}{R(\Omega-\boldsymbol{U}\cdot\boldsymbol{k})}\mathrm{e}^{\mathrm{i}\boldsymbol{k}\cdot\boldsymbol{\xi}-\mathrm{i}\Omega t}; \end{aligned}\right\} \quad (\mathrm{A}\ 6)$$

entropy:

$$\Omega-\boldsymbol{U}\cdot\boldsymbol{k}=0, \quad \tilde{r}=\tilde{r}_s\mathrm{e}^{\mathrm{i}\boldsymbol{k}\cdot\boldsymbol{\xi}-\mathrm{i}\Omega t}, \quad \tilde{p}=\tilde{u}=\tilde{v}=\tilde{w}=0; \quad (\mathrm{A}\ 7)$$

vorticity:

$$\left.\begin{aligned} \Omega-\boldsymbol{U}\cdot\boldsymbol{k}=0, \quad (\tilde{u},\tilde{v},\tilde{w})=(\tilde{u}_s,-\nu^{-1}(\alpha\tilde{u}_s+\beta\tilde{w}_s),\tilde{w}_s)\mathrm{e}^{\mathrm{i}\boldsymbol{k}\cdot\boldsymbol{\xi}-\mathrm{i}\Omega t}, \\ \tilde{p}=\tilde{r}=0. \end{aligned}\right\} \quad (\mathrm{A}\ 8)$$

We denote the pressure amplitudes of the incident and reflected acoustic waves by p_1 and p_2 respectively, and their corresponding η-wavenumbers by ν_1 and ν_2 respectively. Then substituting (A 6)–(A 8) into (A 5), and using the non-dimensional forms of (2.2), we obtain after some manipulation

$$\left(\frac{K_1+K_2\nu_1}{\Omega-\alpha V-\nu_1 V}\right)p_1+\left(\frac{K_1+K_2\nu_2}{\Omega-\alpha U-\nu_2 V}\right)p_2=0,$$

where

$$K_1=\frac{-(\Omega-\alpha U)(\Omega-\alpha U)^2(1+\epsilon^2\mathscr{T}^2)(3-\gamma+(\gamma+1)\epsilon)-(\alpha^2+\beta^2)\epsilon\mathscr{T}^2((\gamma+1)-(\gamma+5)\epsilon))}{(\Omega-\alpha U)^2(1+\epsilon^2\mathscr{T}^2)+(\alpha^2+\beta^2)\epsilon\mathscr{T}^2},$$

$$K_2=\frac{(\gamma+1)(1-\epsilon)\epsilon\mathscr{T}}{(1+\epsilon^2\mathscr{T}^2)^{\frac{1}{2}}}.$$

On substituting the scalings (2.16) into the above, we find that at leading order $|K_1| \gg |K_2|$, $\alpha U \gg |\Omega - \nu_1 V|$, and hence

$$p_1 + p_2 = 0,$$

i.e. condition (3.10). Expressions for other quantities can be obtained similarly. In the asymptotic range (2.16*d, e*) the $\tilde{u}$-, $\tilde{w}$- and $\tilde{r}$-perturbations are dominated by the entropy/shear wave contributions; in particular

$$\tilde{u} \sim \frac{2\tilde{\alpha}\sigma M}{(\tilde{\alpha}^2 - \tilde{\beta}^2)^{\frac{1}{2}}} p_1, \quad \tilde{w} \sim \frac{2\tilde{\beta}\sigma M^2}{(\tilde{\alpha}^2 - \tilde{\beta}^2)^{\frac{1}{2}}} p_1, \quad \tilde{r} \sim \frac{-2\tilde{\alpha}\sigma M^3}{(\tilde{\alpha}^2 - \tilde{\beta}^2)^{\frac{1}{2}}} p_1,$$

where

$$\alpha = Re^{\frac{3}{8}} \mu_{\mathrm{w}}^{-\frac{3}{8}} T_{\mathrm{w}}^{-\frac{9}{8}} M^{-\frac{3}{4}} \tilde{\alpha}, \quad \beta = Re^{\frac{3}{8}} \mu_{\mathrm{w}}^{-\frac{3}{8}} T_{\mathrm{w}}^{-\frac{9}{8}} M^{\frac{1}{4}} \tilde{\beta}.$$

REFERENCES

Blackaby, N. 1990 Ph.D. thesis, University of London.

Blackaby, N., Cowley, S. J. & Hall, P. 1989 To appear as an ICASE report.

Blackaby, N. & Hall, P. 1989 To appear as an ICASE report.

Brown, S. N., Stewartson, K. & Williams, P. G. 1975 Hypersonic self-induced separation. *Phys. Fluids* **18**, 633–639.

DiPrima, R. C. & Hall, P. 1984 Complex eigenvalues for the stability of Couette flow. *Proc. R. Soc. Lond.* A **396**, 75–94.

Gajjar, J. S. B. & Cole, J. W. 1989 The upper branch stability of compressible boundary-layer flows. *Theor. Comp. Fluid Dyn.* **1** (in press).

Gaponov, S. A. 1981 The influence of flow non-parallelism on disturbance development in the supersonic boundary layer. In *Proc. Eighth Canadian Congress of Applied Mechanics.*

Gaster, M. 1974 On the effects of boundary-layer growth on flow stability. *J. Fluid Mech.* **66**, 465–480.

Hall, P. 1983 The linear development of Görtler vortices in growing boundary layers. *J. Fluid Mech.* **130**, 41–58.

Hall, P. & Fu, Y. 1989 Görtler vortices at hypersonic speeds. To appear as an ICASE report.

Hayes, W. D. & Probstein, R. F. 1966 *Hypersonic Flow Theory.* Academic.

Lees, L. 1956 Influence of the leading-edge shock wave on the laminar boundary layer at hypersonic speeds. *J. Aero. Sci.* **23**, 594–600 and 612.

McKenzie, J. F. & Westphal, K. O. 1968 Interaction of linear waves with oblique shock waves. *Phys. Fluids* **11**, 2350–2362.

Mack, L. M. 1969 Boundary-layer stability theory. *Document* 900-277, *Rev. A*, J.P.L. Pasadena.

Mack, L. M. 1984 Boundary-layer linear stability theory. In *Special Course on Stability and Transition of Laminar Flow. AGARD Rep.* 709.

Mack, L. M. 1987 Review of linear compressible stability theory. In *Stability of Time Dependent and Spatially Varying Flows* (ed. D. L. Dwoyer & M. Y. Hussaini). Springer.

Majda, A. 1983 *The Stability of Multidimensional shock fronts.* Memoirs Am. Math. Soc.

Moore, F. K. 1954 Unsteady oblique interaction of a shock waves with a plane disturbance. *NACA TR* 1165.

Moore, F. K. 1963 *Laminar Flow Theory.* Princeton.

Nagamatsu, H. T. & Sheer, R. E. 1985 Critical layer concept relative to hypersonic boundary-layer stability. *AIAA Paper* 85-0303.

Petrov, G. V. 1984 Stability of a thin viscous shock layer on a wedge in hypersonic flow of a perfect gas. In *Laminar-Turbulent Transition* (ed. V. V. Kozlov), *Proc. 2nd IUTAM Symposium.* Springer.

RESHOTKO, E. 1976 Boundary-layer stability and transition. *Ann. Rev. Fluid Mech.* **8**, 311–349.

RIBNER, H. S. 1954 Convection of a pattern of vorticity through a shock wave. *NACA TR* 1164.

SMITH, F. T. 1979*a* On the non-parallel flow stability of the Blasius boundary layer. *Proc. R. Soc. Lond.* A **366**, 91–109.

SMITH, F. T. 1979*b* Nonlinear stability of boundary layers for disturbances of various sizes. *Proc. R. Soc. Lond.* A **368**, 573–589 (also corrections 1980, A **371**, 439–440).

SMITH, F. T. 1989 On the first-mode instability in subsonic, supersonic or hypersonic boundary layers. *J. Fluid Mech.* **198**, 127–153.

SMITH, F. T., SYKES, R. I. & BRIGHTON, P. W. M. 1977 A two-dimensional boundary layer encountering a three-dimensional hump. *J. Fluid Mech.* **83**, 163–176.

STEWARTSON, K. 1964 *Theory of Laminar Boundary Layers in Compressible Fluids.* Oxford University Press.

STEWARTSON, K. 1974 Multistructured boundary layers on flat plates and related bodies. *Adv. Appl. Mech.* **14**, 147–239.